

ELECTROMAGNETIC OPTIMIZATION OF THE FRIB 322 MHz $\beta=0.29$ HALF WAVE RESONATOR*

Ying Xu[†], A. Facco[‡], M. Johnson, S. Miller, J. Popielarski
Facility for Rare Isotope Beams, Michigan State University, MI 48824, U.S.A.

Abstract

A third generation medium velocity Half Wave Resonator (HWR) is in the final stages of design at Michigan State University (MSU) for use in the Facility for Rare Isotope Beams (FRIB) driver linac. The cavity is being designed to deliver 1.9 MV accelerating voltage reliably, with an optimum $\beta=0.29$. The aim is to reduce significantly the peak magnetic field from the first and second generation designs without changing the cryostat design and the linac layout. The design effort optimizes the surface fields for reliable operation but also considers frequency stability and tunability altogether with straightforward fabrication and surface preparation procedures. The electromagnetic and mechanical design started from an existing design and incorporated lessons learned from the MSU developed 322 MHz HWRs for $\beta=0.53$. The third generation cavity has a similar shape but a different design of the beam port flanges which maximizes the available space for the outer conductor.

INTRODUCTION

The Facility for Rare Isotope Beams (FRIB) located at Michigan State University (MSU) is funded by a joint agreement between the US Department of Energy (DOE) and MSU for the advanced study of rare isotope beams [1]. The driver linac for FRIB is a 200 MeV/u superconducting linac with a final beam power of 400 KW [2]. The superconducting linac will be constructed using four types of resonators [3]. This paper will discuss the $\beta=0.29$ half wave resonator shown in Figure 1. Two problems were present in the previous generation cavities design: first, the B_{pk}/E_{acc} value of 10.8 mT/(MV/m) was rather high due to the space available in the cryostat; second, the beam aperture of 30 mm was just the minimum acceptable in that linac section. So the third generation design had the aim of increasing the beam aperture to 40 mm and of reducing B_{pk}/E_{acc} by increasing as much as possible the cavity diameter without changing the available flange-to-flange length in the cryostat.

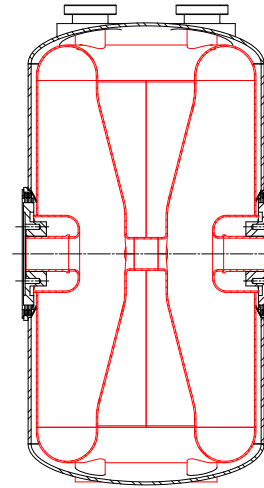


Figure 1: 322 MHz $\beta=0.29$ Half Wave Resonator.

OPTIMIZATION

Current development of half wave RF structures have been extensively described by Conway [4]. Superconducting RF optimizations have been largely limited by trial and error studies where experience plays an extensive part. The optimization process is similar for the $\beta=0.29$ and $\beta=0.53$ half wave resonators with evaluation of each shape with the same purpose of the satisfaction of electromagnetic performance and then on manufacturing and cost [5], and the same optimization parameters are adopted for both half wave resonators. The sketch with notations of optimization parameters is shown in Figure 2. The optimized $\beta=0.29$ and $\beta=0.53$ half wave resonators are shown in Figure 3.

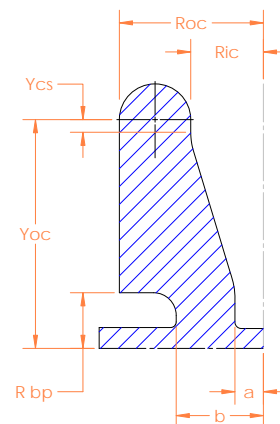


Figure 2: Sketch of optimization parameters.

* Work supported by US DOE Cooperative Agreement DE-SC0000661

[†] xut@nscl.msu.edu

[‡] on leave from INFN Legnaro

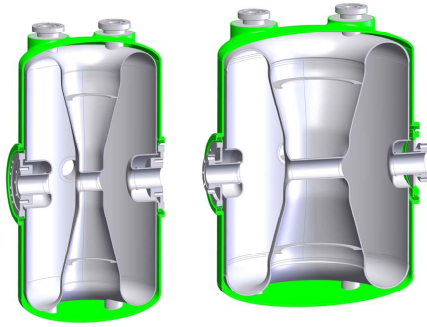


Figure 3: New generation 322 MHz $\beta=0.29$ (left) and $\beta=0.53$ Half Wave Resonator.

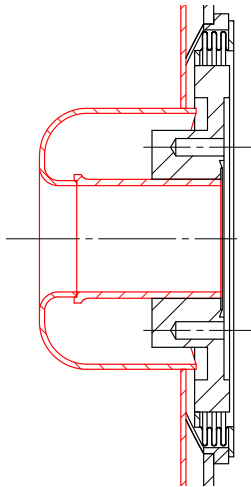


Figure 4: Minimum length flange detail.

In the second generation $\beta=0.29$ resonator design [6], the connection between the short plate and inner conductor is a tangential connection between arc and spline, which causes machining mismatch and welding difficulties. Therefore, in the third generation resonator design, a short cylindrical section between the short plate and inner conductor is introduced, and a minimum 9.5 mm height limit is applied to allow for an electron beam fit up and a smooth transition between parts after welding. However, larger peak magnetic field will be expected for a long cylindrical section. Hence, a 12.7 mm cylindrical section Y_{cs} is implemented in the third generation design. The short plate is optimized to be symmetric along the equator for easier manufacturing and less frequency sensitivity. A conical inner conductor, with a near elliptical cross-section, is implemented for manufacturing convenience where previously a three dimensional spline profile was used. Moreover, the design of the beam port cup includes a flat surface instead of two tangential arcs in the previous generation design, which allows frequency tuning by means of beam port deformation without exceeding plastic limits. Finally, the beam port aperture increases from 30 mm to 40 mm to meet the beam dynamics requirement.

To increase the diameter of the outer conductor and keep the flange to flange length of 324 mm equal to the previous generation, the beam flange design had to be reduced to the minimum possible length. The new flange design can be seen in Figure 4. The cavity to cavity coupling uses Conflat[®] flanges and uses now threaded studs to keep minimum distance between flange surface and cavity outer conductor. The tuner mount location was unchanged. The modifications in geometry parameters between the second and third generation cavities are listed in Table 1.

Table 1: Geometry parameters comparison between 2nd and 3rd generation cavities

Parameter [mm]	2nd	3rd
Beam port aperture	30	40
Outer conductor diameter	228	290
Inner conductor diameter	130	146
Flange to flange distance	324	324

The geometry parameters that have effect on the electromagnetic optimization include: outer conductor radius R_{OC} , inner conductor radius R_{IC} , inner conductor shape, inner conductor cross section profile, short plate height and shape, drift tube length a , beam port cup radius R_{bp} , shape and fillet size, etc. In this paper, we focus on the parameters that make major fields change such as outer conductor diameter, inner conductor diameter, and beam port cup fillet.

Outer conductor diameter

The cavity performance has strong dependence on the outer conductor diameter. The larger the outer conductor diameter, the lower the peak electric and magnetic fields, as shown in Figure 5. The plot also shows that the outer conductor diameter has more effect on the peak magnetic field than on the peak electric field. However, the size of the cavity is limited by the size of the cryomodule. As we mentioned in the previous section, we increased the outer conductor diameter as much as feasible.

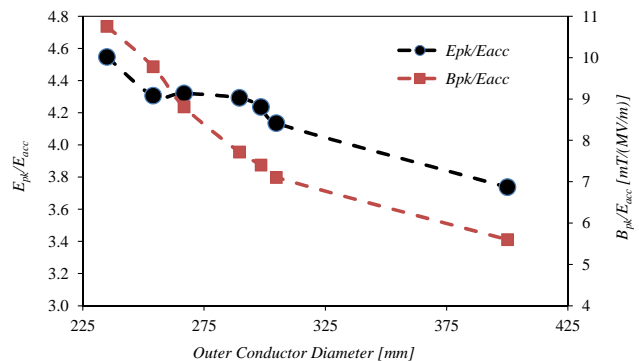


Figure 5: E_{pk} and B_{pk} as a function of outer conductor diameter.

R_{OC}/R_{IC}

The inner conductor diameter, especially the ratio between outer and inner conductor diameters, plays an important role on minimization of the peak magnetic field, and an optimum R_{OC}/R_{IC} for minimum peak magnetic field exists, as indicated in Figure 6.

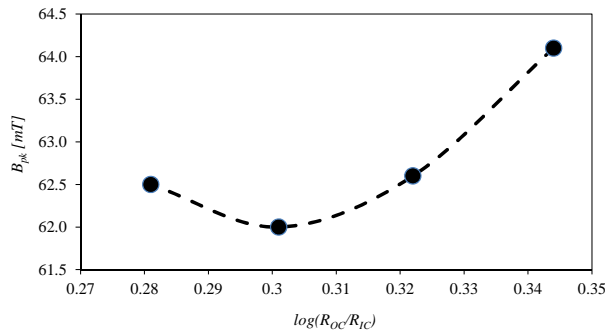


Figure 6: The effect of R_{OC}/R_{IC} on the peak magnetic field.

Other optimization steps

β_{opt} is determined by $b + a$ in Figure 2, which proportionally relates to $\beta\lambda/2$. The peak electric field is lowered by decreasing the curvature of the beam port cup surface and the fillet between inner conductor and drift tube. In addition, the peak electric field reaches its local minimum with the change of drift tube length. The optimization of rinse port fillet requires the fillet large enough such that the peak magnetic field will not be on the rinse port fillet. However, too large rinse port fillet will introduce manufacturing difficulty. Hence, an optimum solution of rinse port and 10 mm fillet was implemented. The adjustment of frequency is done by changing the cavity axial length.

RESULTS

A table of figures of merit compared with those of the second generation cavity is listed in Table 2. For the same accelerating voltage, the third generation design has better electromagnetic performance as well as manufacturing feasibility than the second generation. The surface magnetic and electric fields plot shows that the peak magnetic field is uniformly distributed on the inner conductor, and the peak electric field is on the inner conductor around the drift tube, as shown in Figure 7. The most important result, however, is the reduction of B_{pk}/E_{acc} from 10.8 to 7.7 $mT/(MV/m)$, allowing operation at a much more conservative B_{pk} of 54 mT . This suggested the increase of the cavity specified operation voltage by at least 10%, reducing the required number of cavities in the linac by the same amount with significant cost saving.

Table 2: Figures of merit comparison between 2nd and 3rd generation cavities

Parameter	2nd	3rd
β_{opt}	0.293	0.290
$f [MHz]$	324.0	321.4
$V_a [MV]$	1.90	1.90
$l_{eff} = \beta\lambda [m]$	0.27	0.27
$E_{acc} [MV/m]$	7.04	7.04
E_{pk}/E_{acc}	4.5	4.3
$B_{pk}/E_{acc} [mT/(MV/m)]$	10.8	7.7
$U_0/E_{acc}^2 [J/(MV/m)^2]$	0.180	0.162
$R_a/Q_0 [\Omega]$	200	224
$G [\Omega]$	62	78

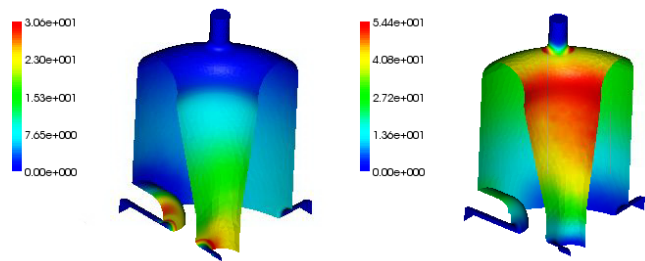


Figure 7: Surface electric (left) and magnetic (right) fields.

CONCLUSIONS

The third generation design of the MSU $\beta=0.29$ cavity for FRIB satisfies the requirements for electromagnetic performance as well as for manufacturing convenience and cost. It has considerably low peak magnetic field, which makes it possible to reach higher accelerating voltage. Moreover, the manufacturing convenience decreases the possibility of cavity defects. Mechanical and thermal analysis is ongoing on the optimized cavity and it is expected to be completed at the end of August 2011. This new cavity design will allow to increase the operation voltage and the cavity transverse acceptance due to the larger beam port aperture without modifying the present cryostat design and the present linac layout.

REFERENCES

- [1] M. Leitner et al., *15th International Conference on RF Superconductivity*, Chicago, IL, 2011, Paper MOPO009.
- [2] W. Hartung et al., in Proceedings, *LINAC 2010: XXV*, Tsukuba, Japan, Paper THP039.
- [3] C. Compton et al., in Proceedings, *LINAC 2010: XXV*, Tsukuba, Japan, Paper THP040.
- [4] Z.A. Conway et al., *PAC 2011*, New York, NY, USA, Paper TUP044.
- [5] S. Miller et al., *15th International Conference on RF Superconductivity*, Chicago, IL, 2011, Paper MOPO051.
- [6] J. Holzbauer et al., *15th International Conference on RF Superconductivity*, Chicago, IL, 2011, Paper MOPO045.